Article:
Erete, JI, Hughes, KJ, Ma, L et al. (3 more authors) (2017) Effect of CO2 Dilution on the Structure and Emissions from Turbulent, Non-premixed Methane-Air Jet Flames. Journal of the Energy Institute, 90 (2). pp. 191-200. ISSN 1743-9671

https://doi.org/10.1016/j.joei.2016.02.004

Effect of CO_2 Dilution on the Structure and Emissions from Turbulent, Non-premixed Methane-Air Jet Flames

James I. Erete, Kevin J. Hughes*, Lin Ma*, Michael Fairweather, Mohamed Pourkashanian* and Alan Williams**,

Energy Research Institute, School of Chemical and Process Engineering,

University of Leeds, Leeds, LS2 9JT, UK

* Present address: Department of Mechanical Engineering, Sheffield University,

Sheffield S10 2TN UK

** Corresponding author: A.Williams@leeds.ac.uk

Abstract

This investigation gives a comparison of the variation of temperature and gas compositions in lifted, turbulent non-premixed methane-air jet flames firing vertically into still air with different carbon dioxide diluent concentrations in the fuel jet. The carbon dioxide mole fraction ranged from 0 to 0.22 and was varied with a fixed jet velocity so that dilution-induced extinction was achieved. The effect of the changes due to this dilution on the post-flame emissions was investigated. Similarly, visual observation of the changes in the flame structure in mixture fraction space at different diluent mole fraction has been studied. An examination of the changes in the flame length, lift-off height, flame temperature, composition, and on the emission indices of the species in the post-flame region were made. They showed an increase in the flame's lift-off height, a decrease in the overall flame length, a reduction in the flame temperature and a reduction in the NOx concentration at various levels of dilution of carbon dioxide in the fuel.

Keywords

Methane, flares, CO_2 dilution, emissions, lift-off

Nomenclature

EI emission index, g kg^{-1}; EINOx, EICO are the emission indices for NOx and CO respectively,

MW_i molecular weight of species i, g

MW_f molecular weight of fuel, g

n number of C atoms in an alkane

X_i mole fraction of species i

$\overline{Y}$ mass fraction

$\overline{Y}_{C,i}$ stoichiometric mass fraction

$\overline{\xi}$ mean mixture fraction

1. Introduction

During crude oil production the associated gas which cannot be further processed either due to cost implications or the volume produced may be flared or re-injected back into the reservoir to increase oil recovery [1]. The use of flaring leads to the formation of carbon dioxide, soot, unburned hydrocarbons, and the emission of other pollutants such as NO [2]. Estimates of CO_2 emissions indicate that about 360 Mt is emitted to the atmosphere annually through flaring and venting [3,4] of which flaring alone accounts for 1.2 % of CO_2 emissions, and the venting of methane accounts for about 4%, globally [5]. Technologies have been developed aimed at reducing emissions and cost [6] but these are limited in their application and consequently gas flaring is still widely used

Flame structure and emissions from methane and natural gas flames have been widely studied in both laboratory-scale and full-scale flares. Methane jets diluted with CO_2 are of interest because it is a combustion product and may be recycled as an inert additive in the air or fuel streams of the flame. The injection of CO_2 into either the oxidiser stream or into the fuel stream is known to affect the flame by reducing the concentration of the reactive species, and reducing the flame temperature. Thus NO_x levels and soot concentrations emitted from the flame are reduced. CO_2 dilution effects have been the subject of various investigations where it has been used as a diluent injected into an oxidiser stream, as air-stream dilution (ASD), as in references [7-13]. Similarly, CO_2 may be injected into the fuel stream as a diluent (fuel-stream dilution) as reported by several researchers. For instance, Kalghatgi studied the effect of CO_2 dilution on the blow-out stability of methane and propane diffusion flames [14]. Briones *et al*. performed a numerical investigation of the effect of fuel dilution on the stability of non-premixed flames [15]. Lock *et al*. investigated the lift-off and extinction characteristics of fuel- and air-stream-diluted methane-air flames [7] and Samanta et al.[16] performed a numerical analysis on the effect of CO_2 dilution on the structure of methane-air diffusion flames.

Previous investigations have shown the effect of CO_2 dilution on flame structure and on the emission indices of NO_x and CO ($EINO_x$ and EICO). However as far as we are aware there has been no previous study of the effect of dilution of the fuel stream on emissions over a broad range of Reynolds numbers, Re. Hence, investigations of the effect of dilution on the EICO and $EINO_x$ over Reynolds numbers ranging from 1,584 to 14,254 are given here. There have been no previous studies on the effect of dilution on the in-flame composition at different axial and radial locations in the flame. This aspect is important because turbulent diffusion flames exhibit non-linear characteristics [17,18]. Similarly, the concentration of chemical species, the temperature, the mixing rate, and the rate of reaction occurring in the flame are useful in characterising the overall structure of the flame [19].

The objectives of this investigation are to visually observe and compare the effect of CO_2 dilution of the fuel-stream on flame structure and on the $EINO_x$ and EICO, over a range of Reynolds numbers. Experimental results on the mean flame temperature, species mass fractions, and flame length and the lift-off height of the jet flames reported.

2. Experimental Methods

The experiments reported in this study were performed in the laboratory in still air in a similar way to that described by Erete et al. [20]. Basically this consist of a Sandia burner burning a methane jet diluted with carbon dioxide with a co-flow of air, metering systems, traversing system, temperature and gas composition measurement equipment, and probing systems. A schematic of the experimental setup is shown in Fig. 1. The fuel jet diameter was 3.25mm, the velocity of the co-flow air was 0.3 m/s and a summary of the test conditions used is given in Table 1.

Flame images were directly captured using a digital camera. The mean visible flame height and the mean visible lift-off height were determined by averaging each of the shots that were captured at 60 fps. This procedure was repeated several times, and averaged to give the mean visible flame length and the mean lift-off distance. The visible flame length for an attached flame used in this study was taken as the axial distance between the jet nozzle exit port rim and the farthest downstream location where the tip of the flame was visible to the human eye. Similarly, for the lifted flame, the lift-off distance was taken as the axial distance along the centre-line of the jet nozzle exit port rim and the downstream plane where the flame just becomes visible i.e., the base of the flame where the flame stabilises independently above the burner jet rim.

Temperature measurements were made using a silica-coated Pt-Pt/13% Rh junction thermocouple to minimise catalytic reactions on its surface. It was mounted in fixed position whilst the burner was moved by means of a 3-D computer controlled traverse which also recorded the position of the thermocouple. The measured wire diameter of the thermocouple was 0.075 mm, with an uncoated bead diameter of 0.16 mm and a coated bead diameter of 0.216 mm. The temperature correction for radiation heat losses was made using the expression by Kaskan [21]. The thermocouple was connected to a data logger.

The in-flame gas samples, which were obtained using an uncooled quartz probe, of a 1 mm orifice diameter passed through a heated sample line into the gas conditioning system to dry the gases before the sample was analysed. This type of probe was used by Drake et al. [23]. The probe was held in a fixed position and the burner moved by the 3-D traverse. The concentrations of CO, CO_2, O_2, NOx and NO were measured using a multi-component gas analyser (Horiba VA-3000). NO_2 was determined by taking the difference between the NO_x and NO measurements [22]. The unburned hydrocarbon was measured using a Flame Ionisation Detector (MEXA 1170 HFID). Each experiment was repeated three times at each location. The uncertainties in the measurements of the mean values of temperature and gas compositions are ±3% and ±5%, respectively.

The burner was placed vertically in the traverse system. Post-flame gas samples were taken using an uncooled quartz probe which was positioned centrally above the tip of the flame. The fuel and the diluent used were commercial-grade methane (CP-Grade 99.5%), and pure CO_2, respectively, which were metered via rotameters before being piped into a mixing chamber. The flow rate of the fuel was kept constant in all the cases while the mole fraction of the diluent in the fuel stream was varied.

Dilution-induced extinction was achieved by fixing the fuel jet velocity, while varying the mole fraction of the diluent, in accordance with the investigation of Lock *et al*. [7], where a uniformly mixed diluent, with mole fraction ranging from 0 to 0.22 CO_2, was added to the fuel stream until

flame extinction occurred. Here it was found that the critical diluent mole fraction leading to extinction was 0.22. However, it was found impractical to measure both the in-flame temperature and the composition of species in the flame when the fuel was diluted with CO_2 above 20% because above this dilution level the flame was highly unstable, thus making reliable measurements difficult to obtained. Therefore, the measurements at a dilution level of 20% examined in this investigation are taken to represent the combustion characteristics of a methane-air jet flame near extinction.

The uniformity of the co-flow air velocity was checked at a number of positions using a hot-wire anemometer. The co-flow velocity was 0.3 m s^{-1}, which was sufficient to minimise disturbances to the flame from movements in the room. This co-flow air velocity was kept constant over all the conditions investigated and was maintained at less than 3% of the fuel jet velocity to avoid any effect of the co-flow air on the flame length and $EINO_x$ levels as discussed by Driscoll *et al*. [24].

3. Results and Discussion

3.1 Flame visualisation

Photographs of some of the jet flames are shown in Fig. 2. From these the luminosity, colour, flame height and the visible lift-off height of each flame were observed. Each flame showed a distinctive colour which changed as the CO_2 concentration was increased; The primary flame zone became a deeper blue colour with increasing concentrations of CO_2 which also made the position of the burner nozzle to be more difficult to be defined. The position of the central jet and the outer jet rim are indicated for each burner in Fig 1 and it can be seen that the flame base is broadened as the CO_2 level is increased. It was also observed that the colours of the flames zones changed as the carbon dioxide was added. Flame A had an orange-yellow colour at the tip of the flame caused by

the incandescenct soot particles but this disappeared as the carbon dioxide level was increased. The primary blue flame zone increased in intensity with carbon dioxide dilution and a bluish-green colour immediately after this zone was observed in flames B and C. Similarly, the deeper bluish colour of the near-extinction flame D, as compared to flames A, B and C, suggests a reduction in the flame temperature. Also, as shown in Fig. 2, the shape of the flame is distinctive in each case, initially being slender at the flame base in the undiluted case, and becoming wider at the base as the CO_2 mole fraction is increased. A further increase in the concentration of the diluent, beyond that used in flame D, caused the base of the flame to oscillate vigorously with no significant increase in the length of the visible flame. At this level of dilution, just before the flame blows out, the intermittency of the flame increased and the flame became very unstable, with further minor increases in the diluent mole fraction leading to complete flame extinction.

3.2 Visual observation of the flame length and lift-off height

The visually-determined overall flame height and the lift-off height at different dilution levels are shown in Fig. 3. The results show that while there was a decrease in the flame length, there was an associated increase in the lift-off height of the jet flames with increasing levels of diluent in the flame. The measured lift-off heights in these flames are consistent with the linear relationship between the jet inlet velocity and the lift-off height observed by Chen *et al*. [18]. The shortening of the length of the visible flame with increasing diluent mole fraction (flames B, C and D) is because the combustible component of the fuel is reduced leading to a decrease in the flame temperature, and reduction in the flame's residence time, reaction rate, and in the time available for mixing and combustion of the fuel. A further increase in the diluent mole fraction leads to a further shortening of the flame and extinction.

It was observed that although the difference in the level of dilution between flames C and D was quite small, even this slight increase (2 vol. %) in dilution leads to a disproportionately greater lift-off height and shorter flame length, which is consistent with the observations of Lock *et al*. [7]. In particular, small increases in this length were found at low dilutions, followed by more significant increases in the lift-off height at greater dilution levels near the blow-out condition. This was the main reason why flame temperatures and species compositions were not measured in flame D, due to the high levels of oscillation at the flame base., Similarly, it should be noted that the flame lift-off height for diluted fuels is also affected by factors such as the aerodynamics of the jet flame [19] and the co-flow air velocity [26].. However, this investigation suggests that, for the flames studied, the lift-off height was increased by the addition of the diluent alone. This is because the jet and co-flow velocities remained unchanged across all the jet flames considered, but the lift-off height was found to increase with increasing dilution of the fuel with CO_2. This dilution causes a reduction in both the mass fraction of the reactant and the length of the heat-release zone, with an associated reduction in the reaction rate at the flame's leading edge which changes the flame propagation speed, thereby leading to stabilisation of the flame further downstream at increased levels of dilution.

3.3 Temperature profiles

The maximum mean temperature recorded in the flames for 0, 0.1 and 0.2 CO_2 mole fractions were 1925K, 1890K and 1858K, respectively, at a normalised axial position of y/d=32.3, indicating the main region of combustion in the flames, as shown in the mean temperature profiles in Fig. 4. The variation in the maximum temperature indicates that an increase in the dilution of the fuel with CO_2 leads to a reduction in the flame temperature, as expected. This may be explained by the combined effect of dilution of the reactive species in the flame zone and heat capacity effects.

Similarly, it was also observed that the flames exhibited an axially symmetric trend in temperature, as anticipated, with a double peak structure which was largest in the undiluted flame (flame A), in the near-nozzle reactive region of this flame, while the peaks became less pronounced in flame C, as shown in the temperature profiles in Fig. 4. This decrease in peak temperatures as the diluent mole fraction increased is due to a decrease in the concentration of radical species in the flames, and the greater entrainment of air into the jet flame. In addition, the dilution of the fuel led to a 35 K difference in the peak mean temperature between the undiluted flame and the flame with 10% CO_2 dilution, while the difference in peak temperature between the flame with 20% fuel-stream dilution and that with no dilution was 67 K, indicating the significant impact of dilution of the fuel on the flame temperature, as well as on the lift-off height of the flame as previously noted. One of the practical implications of this effect of dilution of the fuel stream is that the lower flame temperatures can aid the durability of flare-tips when used in full-scale flares.

3.4 CH_4, O_2, N_2, CO, CO_2 and H_2O composition profiles

As the fuel stream diluent mole fraction is increased in lifted flames the residence time of the flame decreases, the flame length decreases and the lift-off height increases causing the reaction zone to move downstream. More air is entrained in the fuel stream with increasing diluents levels and the overall effect is a decrease in the flame temperature until flame extinction occurs. [7]. These effects result in changes in flame structure and geometry and the emission indices.

Plots of the mass fraction against mixture fraction for the reactant (CH_4, O_2 and N_2), an intermediate (CO), and the product (CO_2 and H_2O) at six different axial locations in the flames are shown in Figs 5 to 8. The mean mixture fraction, $\bar{\xi}$, was calculated based on the carbon atom balance from the experimental data generated for the fuel, CO and CO_2 using the expression employed by Masri and Bilger [26]:

$$\bar{\xi} = \left[(12/16.032)\bar{Y}_{CH_4} + (12/28)\bar{Y}_{CO} + (12/44)\bar{Y}_{CO_2}\right]/\bar{Y}_{C,i} \quad (1)$$

The mass fraction of each species at any given mean mixture fraction depends on the location in the flame where the measurement was made and the intensity of the rate of mixing at that location, with the mixing rate increasing with upstream location in the flame due to the chemical kinetic effects [26]. Similarly, at different dilution levels of CO_2, there is a variation in the maximum fuel mass fraction measured on the flame's centreline at downstream locations in the flame, where in mixture fraction space this varies from 0 in the air stream to 1 in the pure fuel stream, with intermediate values in partially-mixed streams [23]. For example, moving downstream, from y/d=32.3 to y/d=125.5, the mass fraction of the reactant decreases. The mass fraction of the reactant in the near-burner zone is relatively high because this is the closest region to the jet nozzle, where the fuel has just issued, although, because the flames are lifted from the burner, a high level of air entrainment is expected in this region. Plots of the species mass fraction versus mixture fraction show that at different levels of dilution, the reactant, the intermediate and product species tend towards the fuel-lean side of stoichiometric as the diluent mole fraction is increased. This starts from y/d=63.1 at a diluent concentration of 10%, and becomes more obvious at a dilution of 20% CO_2, where the mass fraction of the species becomes leaner as the flame approaches extinction, indicating that just before blow-out the flame becomes very lean due to the thermal, chemical and dilution effects of the diluent, in line with the investigations of Lock *et al*. [7]. In Fig. 5, the maximum mass fraction of CH_4 was recorded on the fuel-rich side of stoichiometric, and in the near-burner zone in all cases investigated, as expected. This zone is closest to where the fuel has just issued, with the mass fraction of CH_4 subsequently decreasing with downstream and radial distance in the flame. Of particular note is the sudden drop in the mass fraction of the fuel at y/d=63.1 in the diluted cases. This can be explained by the reduction in the concentration of the reactant species due to the addition of CO_2 leading to a decreased reaction rate, and hence lower measured mass fraction of this species at that location.

In Fig. 6, and for all cases investigated, the maximum mass fraction of oxygen was observed at the following locations: upstream of the base of the visible flame, at downstream locations above the tip of the visible flame, and at radial locations away from the flame, as might be expected. In Fig. 7, the mass fraction of the product species increase downstream from y/d=32.3 to y/d=157.8 at all levels of dilution, while in Fig. 8, the mass fraction of the intermediate species, CO, increases downstream between y/d=1.5 and y/d=63.1, peaking at the latter location before decreasing further downstream. The results for the CO and CO_2 mass fractions show that in the undiluted case, the peak concentrations of CO and CO_2 were recorded on the fuel-rich and fuel-lean sides of stoichiometric, respectively. However, in the diluted cases, the dilution of the fuel with CO_2 leads to higher CO_2 mass fractions on the fuel-rich side of stoichiometric, with increasing levels of CO_2 at higher diluent mole fraction observed in the near-burner zone, at y/d=1.5, and relatively lower levels at downstream locations in the flame. In the undiluted case, the peak CO mass fraction lies on the fuel-rich side of stoichiometric, while in the diluted cases, the peak CO mass fraction in flame B decreases gradually towards stoichiometric before crossing over to the lean-side, while flame C remains on the lean side of stoichiometric at most locations in the flame. This is expected because CO formation is favourable in locations of relatively low air concentration, high fuel concentration, and low temperature which consequently reduce the rate of reaction for the oxidation of CO to CO_2. Similarly, fuel-stream dilution with CO_2 favours lower temperatures, and these lower temperatures also promote the formation of CO as a result of quenching of the oxidation reaction, thereby leading to higher local CO levels in the flame. In addition, by adding CO_2 to the fuel stream, the CO mass fraction is increased as the level of dilution is increased across the flames. This is expected because the reaction of H with CO_2 to produce CO and OH favours a higher mass fraction of CO and OH due to the chemical effects of CO_2 in the fuel stream. The effect of this dilution also leads to a change in the flame's stoichiometry, causing a decrease in the flame's local and global residence times [27], and with the chemistry of the flame being skewed away from stoichiometric.

3.5 NO, NO_2 and NO_x composition profiles

The dilution of fuel with CO_2 leads to a reduction in the concentration of NO and, to a lesser extent, on the local concentration of NO_2. NO is the dominant nitrogen oxide pollutant species that is emitted by hydrocarbon flames. Although these pollutants do not take part directly in the combustion process they are linked to the main combustion process. In the previous section, it was shown that an increase in the fuel-stream dilution leads to a reduction in the flame temperature. Consequently, this reduction in temperature further aids the reduction of NO_x levels in the flame. In Figs 9 and 10, the effect of CO_2 dilution on NO and NO_2 respectively, is shown in plots of the local concentration of the pollutant in ppm versus the mixture fraction. In all cases, the maximum concentration of these pollutants lies on the lean side of stoichiometric. This is because higher fuel concentrations lead to higher flame temperatures, and an increase in O_2 and N_2 concentrations available within the flame zone enhances NO levels via the Zeldovich mechanism [28]. However, when the fuel stream is diluted with CO_2, there is a reduction in the reactant mass fraction in regions of high temperature within the flame, thereby leading to losses of radical species, lower reaction rates and temperatures, which in turn lead to lower NO levels. This is shown where the effect of increased dilution of the fuel leads to a reduction in the fuel concentration, as in Fig. 5, and a reduction in the peak temperature, causing the reaction zone to move downstream and consequently the lower concentrations of NO and NO_2 measured in the flame. In increasing order of CO_2 dilution in the three flames investigated, the peak concentrations of NO in ppm were 23.4, 19.9 and 16.7, and of NO_2 were 4.7, 5.8 and 5.9. This implies that diluent CO_2 mole fractions of 0.1 and 0.2 lead to 15% and 29% decreases, respectively, in NO concentration, and 23% and 26% increases in NO_2 concentrations, respectively, demonstrating that a decrease in NO concentrations leads to an increase in NO_2 concentrations as the diluent mole fraction is increased. The effects of dilution and the consequent lower flame temperatures lead to lower soot volume fractions and lower NO_x concentrations in a flame. The percentage of NO_x that is NO_2 in the

post-flame region ranges from about 7% - 40% [22], and peak concentrations of NO_2 have been found to be in downstream regions of a flame, and at post-flame locations where rapid cooling or dilution occurs, which also coincides with those locations where radicals formed in the peak-temperature regions of a flame are rapidly cooled.

NO_2 has often been neglected in some combustion processes [29] because of its relatively low concentration in hydrocarbon flames, as compared to NO, yet NO_2 is more toxic than NO [30], and NO is ultimately converted to NO_2 in the atmosphere [24]. As shown in Fig. 10, the peak concentration of NO_2 in both the diluted and undiluted cases occur at a downstream location of y/d=93.9, and does not vary significantly between flames, irrespective of the level of CO_2 dilution of the fuel stream. NO_2 formation occurs mainly via the oxidation of NO with the HO_2 radical in the flame zone at short residence times via the reaction of NO and HO_2 to yield NO_2 and OH [30, 31], although NO_2 may also be formed via the reaction of NO with other species such as O_2, O and OH in the flame zone. In hydrocarbon flames, NO_x is generally made up of approximately 80% NO, or higher [32], while the remainder is NO_2, implying that NO concentration profiles should follow NO_x profiles closely because of the higher contribution of NO in NO_x than NO_2. In the cases investigated, only small concentrations of NO_2 were recorded in the CH_4 flames, as expected because of chemical kinetic reasons. As a result of the relatively high temperature the NO-NO_2 conversion is very slow until the combustion products cool. In Fig. 10, it can be seen that the in-flame NO_2 concentration increases slightly as the diluent CO_2 mole fraction increases.

3.6 Effect of fuel-stream dilution on EINO_x and EICO

Factors such as the composition of the reactants, the flame structure, the flame temperature, and the rate of chemical reaction taking place in upstream portions of the flame determine the level of

post-flame pollutant species emissions. These species may be reported as an emission index, which is a measure of the mass of species emitted (g) per mass of fuel combusted (kg), and is expressed mathematically as:

$$EIX_i(g/kg) = nX_i / X_{CO_2} \times MW_i / MW_f \times 1000 \quad (2)$$

where *n* is the number of carbon atoms in an alkane [33]. The emission of NO_x from fossil fuels is in the form of NO which is oxidised to NO_2 in the atmosphere and in exhaust systems [34], therefore the emission index of NO_x is reported as the equivalent of that of NO_2, where the molecular weight of NO_2 is used in calculating the $EINO_x$ [24, 27]. Plots of the emission indices of NO_x and CO at different diluents CO_2 mole fractions are presented in Figs. 11 and 12, respectively. It was observed that for all the Reynolds numbers investigated, increasing the mole fraction of CO_2 in the fuel led to a decrease in the $EINO_x$, and an increase in EICO. For the $EINO_x$, the dilution led a decrease in the concentration of reactive species, and lower flame temperatures, leading to a lower $EINO_x$. Similarly, higher diluent concentrations lead to an increase in the EICO in the post-flame location of the flame. This can be explained by the low temperatures and the shorter flame zone residence times which reduce the rate of the oxidation of CO to CO_2 and leading to higher EICO levels, which is consistent with the observations of Turns and Bandaru [35].

4. Conclusions

The effect of CO_2 dilution on turbulent, non-premixed CH_4-air flames firing vertically in still air has been investigated. From examination of the consequent changes in the flame temperature, stability, species mass fractions and emission indices of the jet flames, the results show a significant influence of CO_2 dilution of the fuel stream, and the following conclusions are made:

- Results for species mass fractions in mixture fraction space are effective in visualising changes in the flame structure at different levels of diluent CO_2 mole fraction.

- The luminosity of the flame decreases with an increase in diluent concentration.
- A significant increase in the flame lift-off height, and a decrease in the overall visible flame length, is apparent with increasing CO_2 dilution levels.
- Flame blow-out is sensitive to the level of CO_2 dilution.
- An increase in the dilution levels of CO_2 leads to a decrease in the flame temperature due to a reduction in the concentration of radical species in the flame, with an increase in the heat capacity of the unburned mixture similarly affecting flame temperatures.
- CO_2 is an effective diluent for not only suppressing soot formation, but also for the reduction of flame temperature and NO_x concentration.
- A decrease in NO concentration leads to an increase in NO_2 concentration as the diluent mole fraction is increased. CO_2 dilution of the fuel stream at 0.1 and 0.2 mole fraction therefore leads to a 23% and 26% increase, respectively, in NO_2 concentration, and a 15% and 29% decrease, respectively, in NO concentration.
- CO_2 dilution leads to an increase in the EICO and a decrease in the $EINO_x$ at Reynolds number ranging from 1,584 to 14,254.

Acknowledgements

The authors wish to acknowledge the financial support from the Niger Delta Development Commission, and the contributions of Professor D Ingham, Dr. C Atako, K Scott, P Crosby and G Bhogal.

References

[1] International Petroleum Industry Environmental Conservation Association (IPIECA) and American Petroleum Institute (API). Oil and Natural Gas Industry Guidelines for Greenhouse Gas Reduction Projects, Part III: Flare Reduction Project Family; 2009.

[2] McEwen, J.D.N., Johnson, M.R. Black carbon particulate matter emission factors for buoyancy-driven associated gas flares. J Air Waste Manag. Assoc. 2012; 62: 307-21.

[3] Associated Gas Utilization in Russia: Issues and Prospects. Annual Report, Issue 3, Moscow, 2011.

[4] Oliver, J.G.J., Janssens-Maenhout, G., Muntean, M., Peters, J.A.H.W. Trends in Global CO_2 Emissions. 2013 Report, The Hague: PBL Netherlands Environmental Assessment Agency; Ispra: Joint Research Centre.

[5] International Association of Oil and Gas Producers, Flaring and Venting in the Oil and Gas Exploration and Production Industry: An overview of purpose, quantities, issues, practices and trends. Report number 2.79/288, January 2000.

[6] Johnson, M.R., Coderre, A.R. Opportunities for CO_2 equivalent emissions reductions via flare and vent mitigation: A case study of Alberta, Canada. Int. J. Greenh. Gas Control 2012; 8: 121-31.

[7] Lock, A., Briones, A.M., Aggarwal, S.K., Puri, I.K., Hegde, U. Liftoff and extinction characteristics of fuel- and air-Stream-diluted methane-air flames. Combust Flame 2002; 149: 340-52.

[8] Lock, A., Aggarwal, S.K., Puri, I.K., Hegde, U. Suppression of fuel and air stream diluted methane-air partially premixed flames in normal and microgravity. Fire Safety J. 2008; 43: 24-35.

[9] Lock, A., Aggarwal, S.K., Puri, I.K. Effect of fuel type on the extinction of fuel and air stream diluted partially premixed flames. Proc. Combust. Inst. 2009; 32: 2583-90.

[10] Takahashi, F., Linteris, G.T., Katta, V.R. Extinguishment of methane diffusion flames by carbon dioxide in co-flow air and oxygen-enriched microgravity environments. Combust. Flame 2008; 155: 37-53.

[11] Guo, H., Min, J., Galizzi, C., Escudie, D., Baillot, F. A numerical study on the effects of CO_2/N_2/Ar addition to air on lift-off of a aminar CH_4 /air diffusion flame. Combust. Sci. Tech. 2010;182: 1549-63.

[12] Min, J., Baillot, F. Experimental investigation of the flame extinction processes of non-premixed methane flames inside an air coflow diluted with CO_2, N_2 or Ar. Combust. Flame 2012; 159: 3502-17.

[13] Oh, J., and, D. The effect of CO_2 addition on the flame behaviour of a non-premixed oxy-methane jet in a lab-scale furnace. Fuel 2014; 117: 79-86.

[14] Kalghatgi, G.T. Blow-out stability of gaseous jet diffusion flames. Part 1: In still air. Combust. Sci. Tech. 1981; 26: 233-39.

[15] Briones, A.M., Aggarwal, S.K., Katta, V.R. A numerical investigation of flame lift-off, Stabilization and blowout. Phys. Fluids 2006; 18: 043603.

[16] Samanta, A., Ganguly, R., Datta, A. Effect of CO_2 dilution on flame structure and soot and NO formations in CH_4-Air nonpremixed flames. J. Eng. Gas Turbines Power 2010; 132: 124501-5.

[17] Jeng, S-M., Lai, M-C., Faeth, G.M. Nonluminous radiation in turbulent buoyant axisymmetric flames. Combust. Sci. Tech. 1984; 40: 41-53.

[18] Chen, T. H., Goss, L.P., Talley, D. G., Mikolaitis, D. W. Dynamic stabilization zone structure of jet diffusion flames from lift-off to blowout. J Prop. Power 1992; 8: 548-52.

[19] Gollahalli, S.R., Zadeh, G.K. Flame structure of attached and lifted jet flames of low-calorific-value gases. Energy Sources 1985; 8: 43-66.

[20] Erete, J.I., Aboje, A.A., Hughes, K.J., Ma, L., Pourkashanian, M., Williams, A. An investigation of methane and propane vertical flares. J. Energy Inst. 2015; 85: 1-14.

[21] Kaskan, W. E. The dependence of flame temperature on mass burning velocity, Proc. Combust. Inst. 1957; 6: 134-43.

[22] Turns, S. R. Lovett, J. A. Measurements of oxides of nitrogen emissions from turbulent propane jet diffusion flames. Comb. Sci. Tech. 1989; 66: 233-49.

[23] Drake, M.C., Correa, S.M., Pitz, R.W., Shyy, W., Feninmore, C.P. Superequilibrium and thermal nitric oxide formation in turbulent diffusion flames. Combust. Flame 1987; 69: 347-65.

[24] Driscoll, J.F., Chen, R-H., Yoon, Y. Nitric oxide levels of turbulent jet diffusion flames: Effects of residence time and Damköhler Number. Combust. Flame 1992; 88: 37-49.

[25] Chen, T.H, Goss, L.P. Flame Lifting and Flame/Flow Interactions of Jet Diffusion Flames. AIAA 1989; 89-0156.

[26] Masri, A.R. and Bilger, R.W. Turbulent non-premixed flames of hydrocarbon fuels near extinction: Mean structure from probe measurements. Proc.Combust.Inst. 1986; 21: 1511-20.

[27] Turns, S.R., Myhr, F.H., Bandaru, R.V., Maund, E.R. Oxides of nitrogen emissions from turbulent jet flames: Part II-Fuel dilution and partial premixing effects. Combust. Flame 1993; 93: 255-69.

[28] Turns, S.R., Myhr, F.H. (1991) Oxides of nitrogen emissions from turbulent jet flame: Part 1 – Fuel effects and flame radiation. Combust. Flame 1991; 87: 319-35.

[29] Zhuang, J., Leuckel, W. Formation of nitrogen dioxide in combustion processes. International Gas Research Conference. Industrial Utilization and Power Generation 1998; 5: 349-60.

[30] Homma, R., Chen, J.-Y. Combustion process optimization by Genetic Algorithms: Reduction of NO_2 emission via optimal post-flame process. Proc. Combust. Inst. 2000; 28: 2483-9.

[31] Merryman, E.L., Levy, A. Nitrogen oxide formation in flames: The roles of NO_2 and fuel nitrogen. Proc. Combust Inst. 1974; 15: 1073-83.

[32] Namazian, M., Kelly, J.T., Schefer, R.W. Simultaneous NO and temperature imaging measurements in turbulent nonpremixed flames. Proc. Combust. Inst. 1994; 25: 1149-57.

[33] RØkke, N.A., Hustad, J.E., SØnju, O.K. A study of partially premixed unconfined propane flames. Combust. Flame 1994; 97: 88-106.

[34] Pourkashanian, M., Yap, L.T., Howard, L., Williams, A., Yetter, R.A. Nitric-oxide emissions scaling of buoyancy-dominated oxygen-enriched and preheated methane turbulent-jet diffusion flames. Proc. Combust. Inst. 1998; 27: 1451-1460.

[35] Turns, S.R., Bandaru, R.V. Carbon monoxide emissions from turbulent nonpremixed jet flames. Combust. Flame 1993; 94: 462-8.

Table 1. Test conditions for the present investigation.

Jet Flame	A	B	C	D
Fuel concentration / Vol. %	100	90	80	78
Diluent Concentration / Vol. %	0	10	20	22

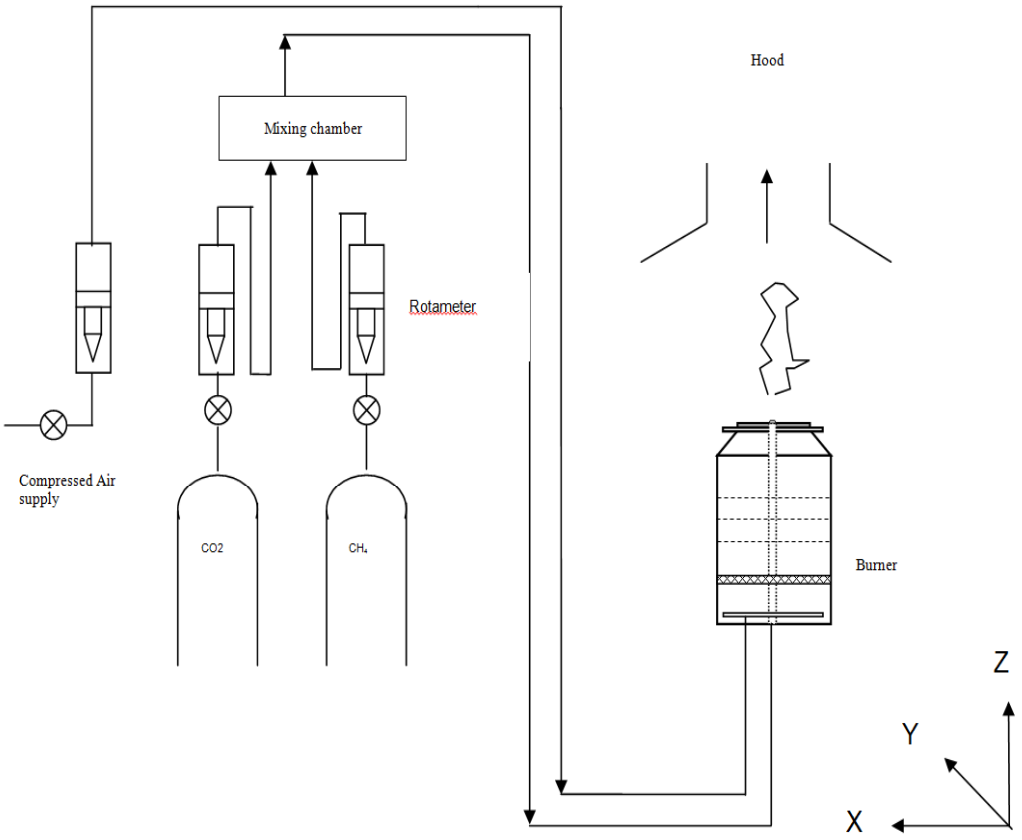

Fig. 1. Schematic diagram of the experimental equipment.

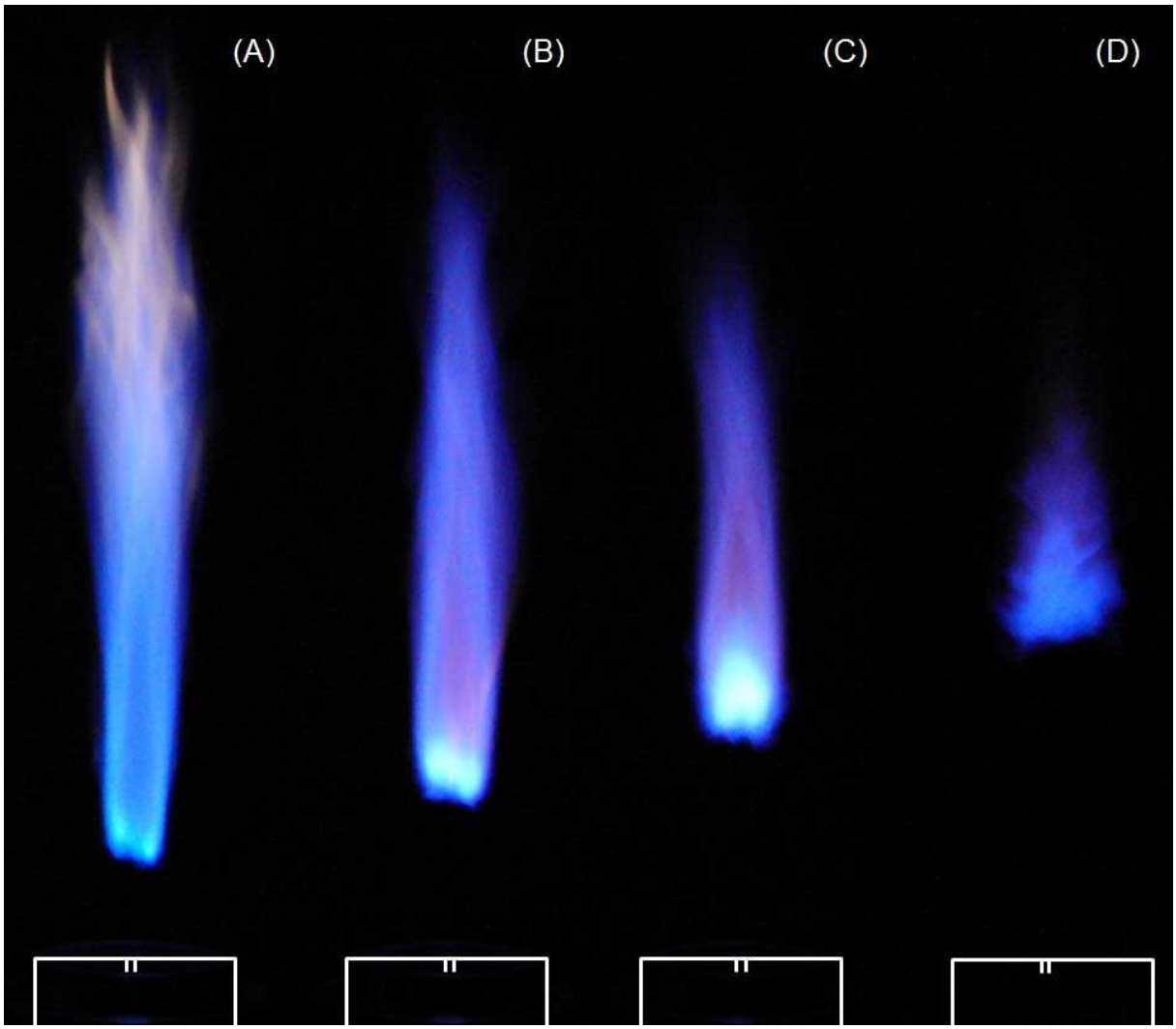

Fig. 2. Photographs of methane jet flames showing the effects of increasing CO2 dilution on flames A, B, C and D respectively. The jet nozzle and the burner rim are shown

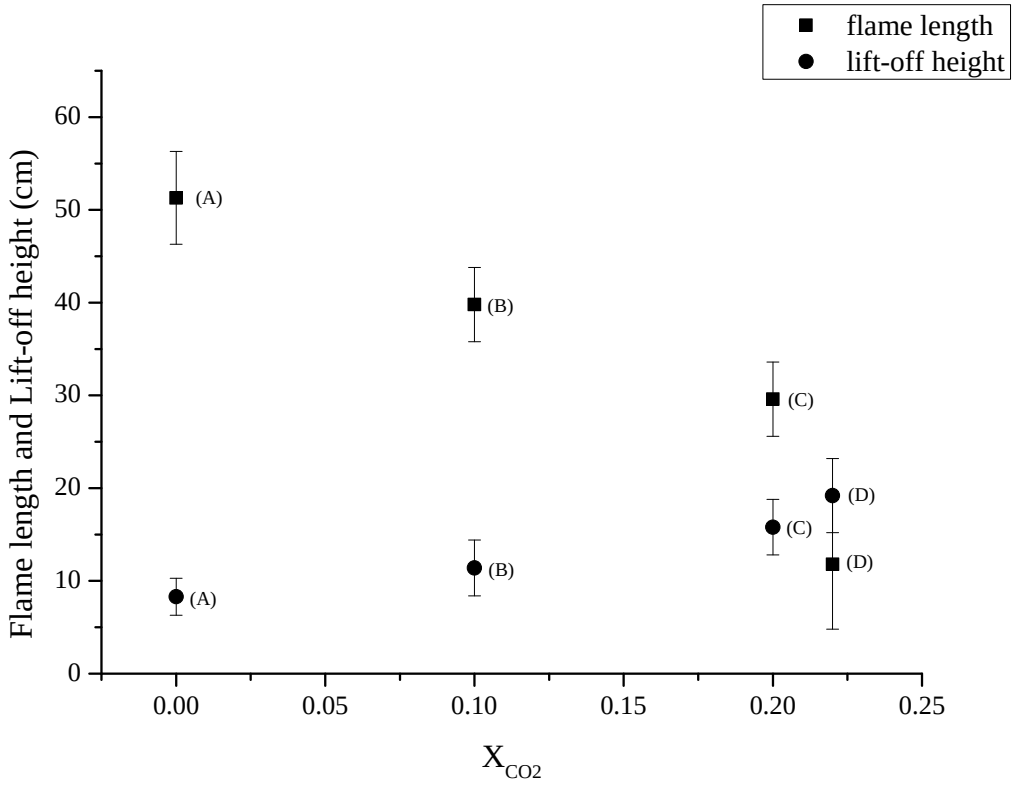

Fig. 3.Changes in the visually-determined flame height and lift-off height with increases in diluent concentration for flames A, B, C and D.

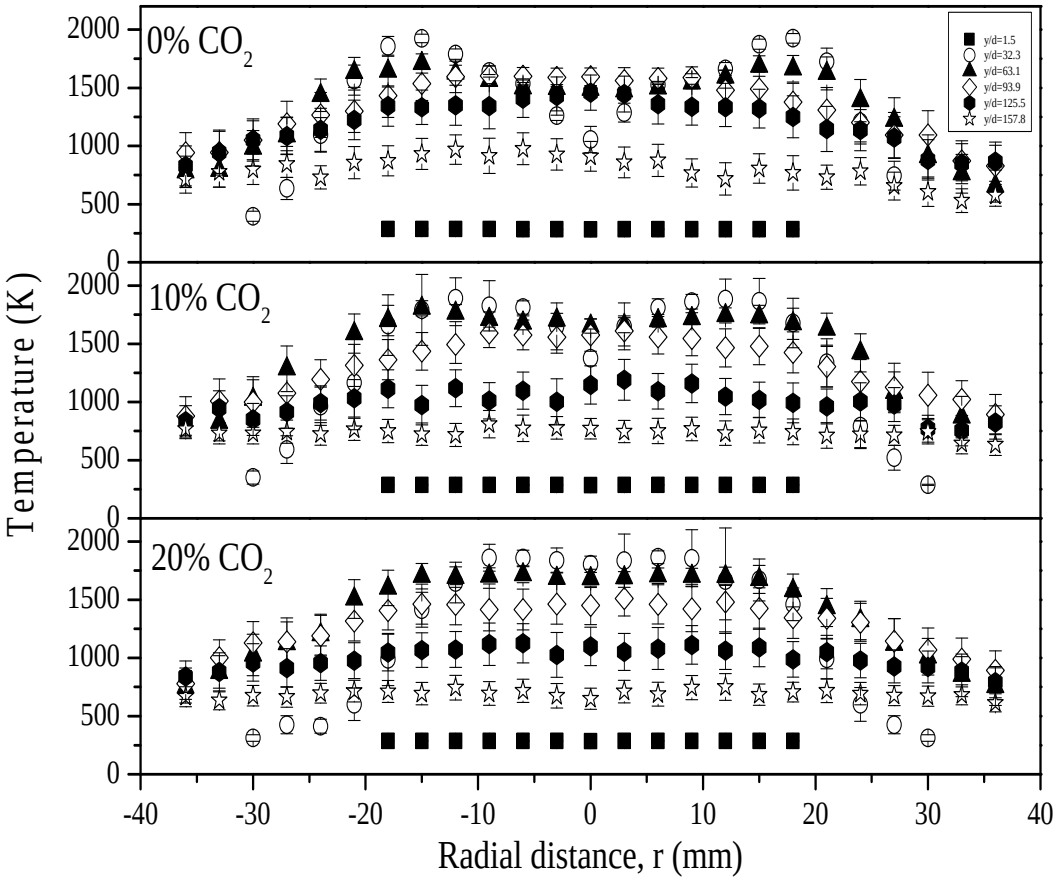

Fig. 4. Mean temperatures for the three jet flames investigated (flames |A, B and C) as a function of radial position and downstream distance.

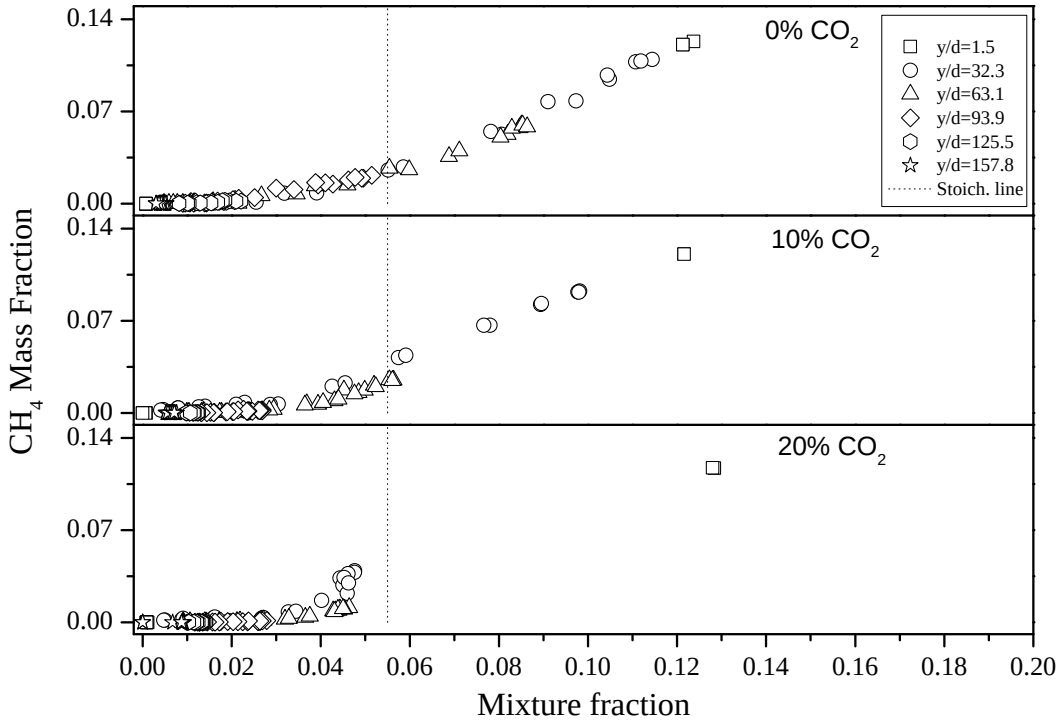

Fig. 5. CH_4 mass fraction versus mixture fraction plots for flames A, B and C, corresponding to diluent CO_2 mole fractions of 0, 0.1 and 0.2 respectively.

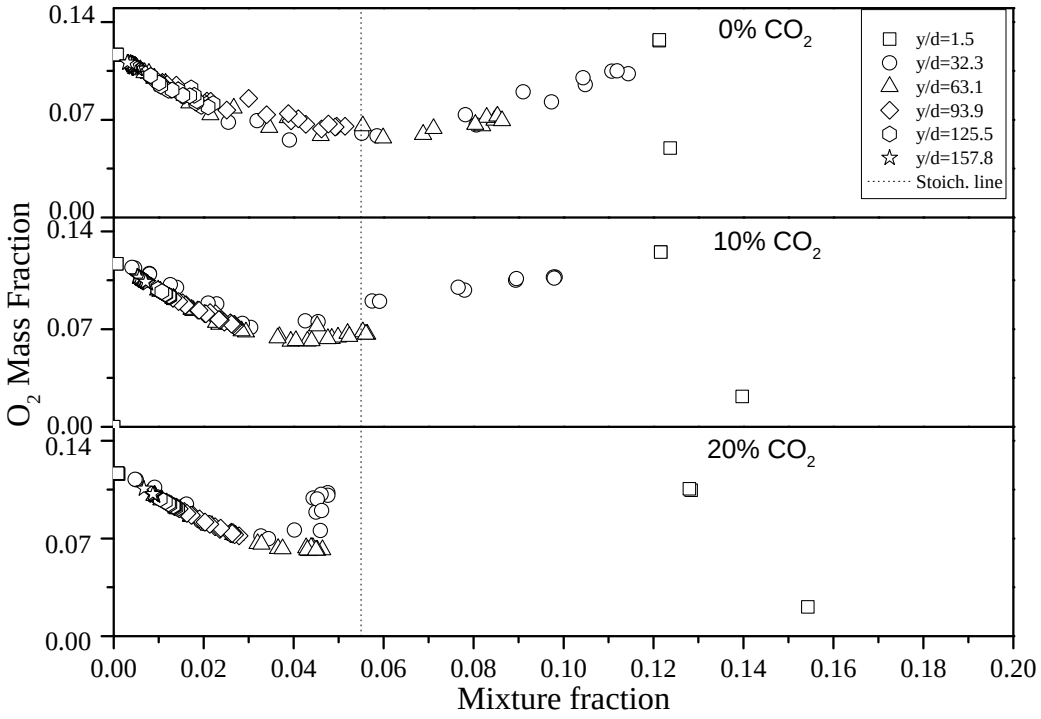

Fig. 6. O_2 mass fraction versus mixture fraction plots for flames A, B and C, corresponding to diluent CO_2 mole fractions of 0, 0.1 and 0.2 respectively.

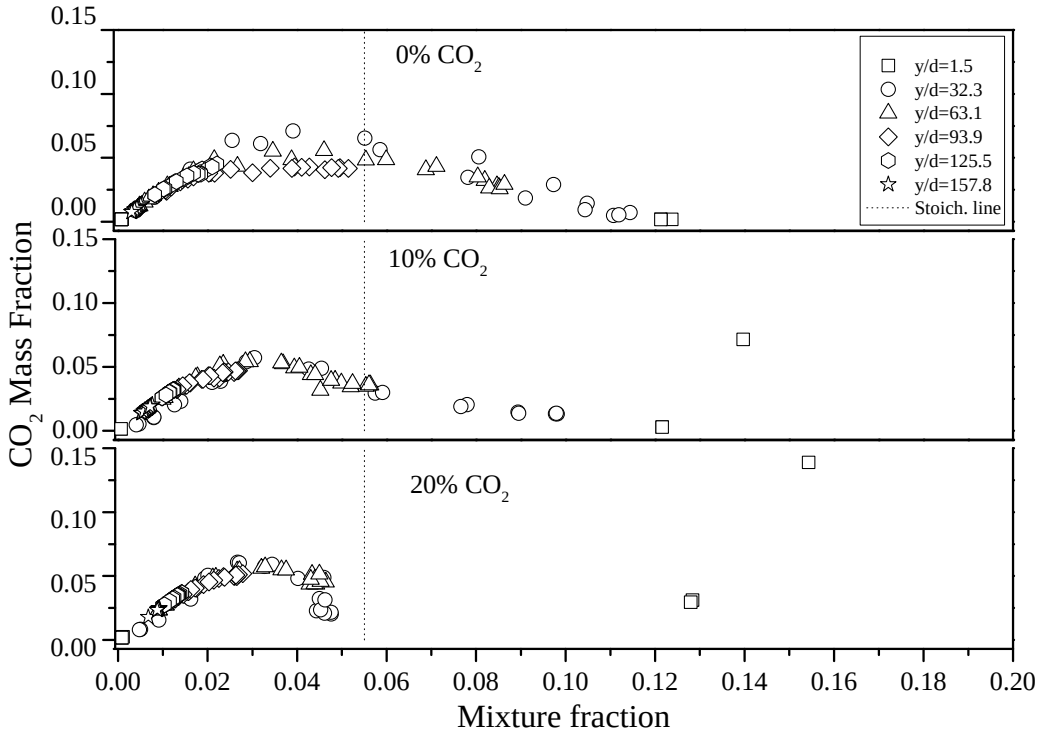

Fig. 7. CO_2 mass fraction versus mixture fraction plots for flames A, B, and C, corresponding to diluent CO_2 mole fractions of 0, 0.1 and 0.2 respectively.

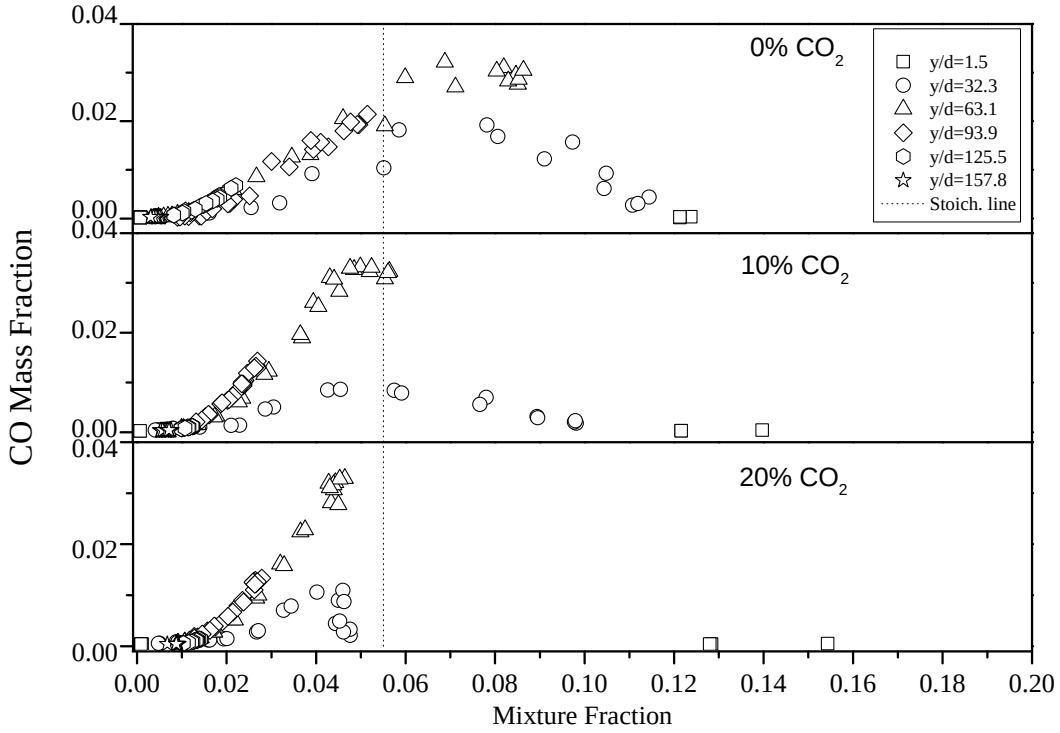

Fig. 8. CO mass fraction versus mixture fraction plots for flames A, B, and C, corresponding to diluent CO_2 mole fractions of 0, 0.1 and 0.2 respectively.

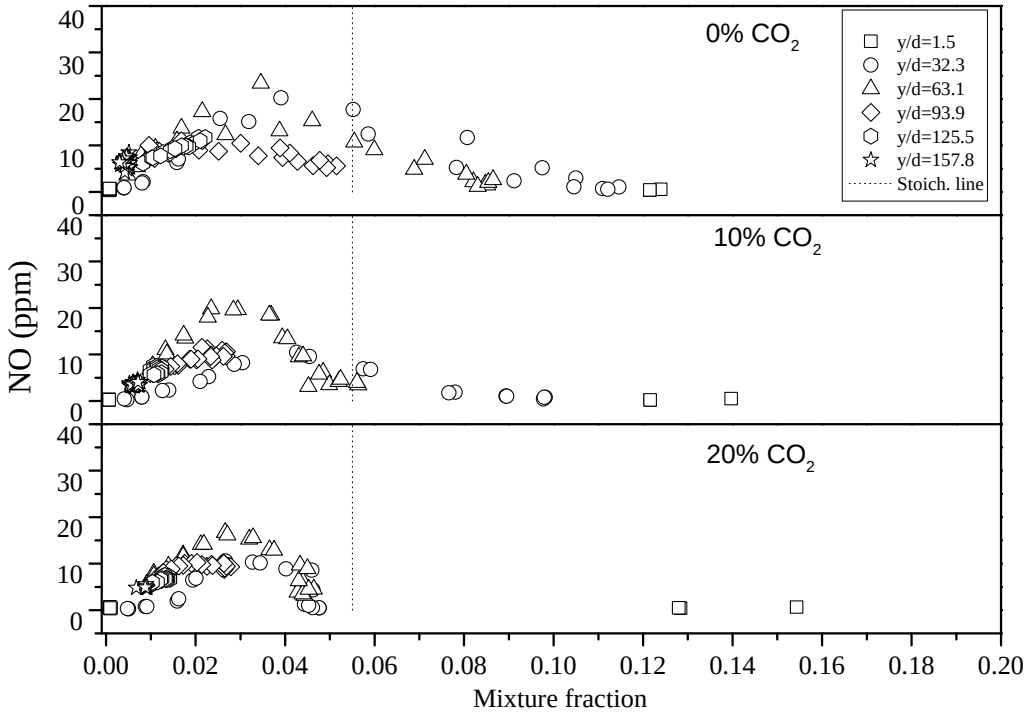

Fig. 9. NO concentration versus mixture fraction plots for flames A, B and C, corresponding to diluent CO_2 mole fractions of 0, 0.1 and 0.2 respectively.

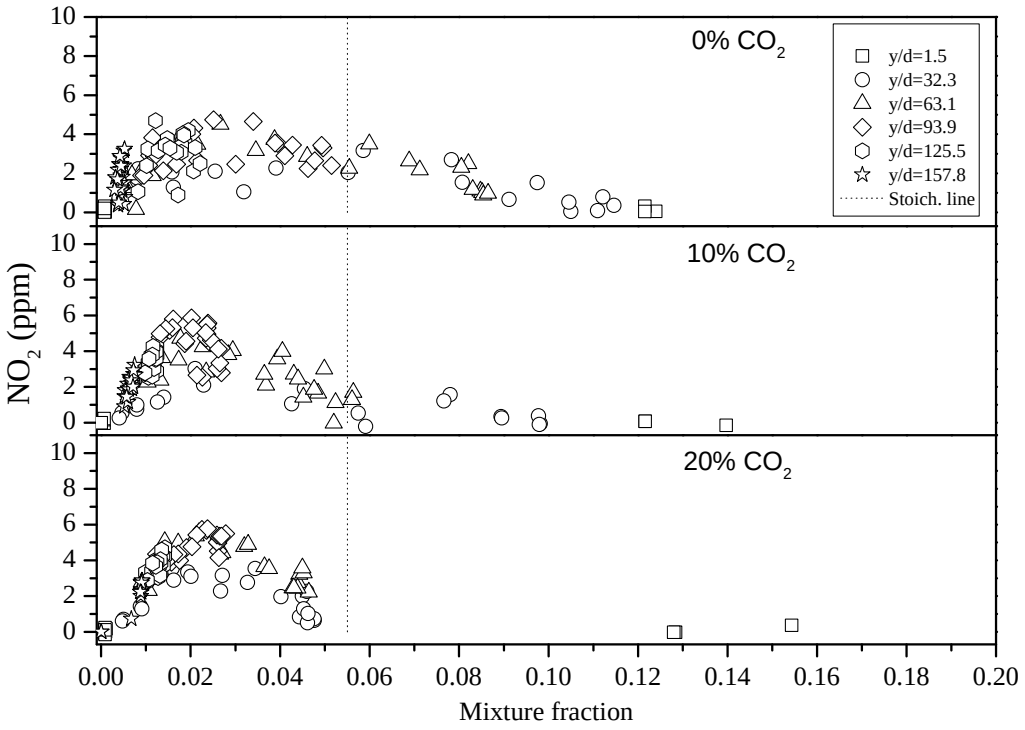

Fig. 10. NO_2 concentration versus mixture fraction plots for flames A, B and C, corresponding to diluent CO_2 mole fractions of 0, 0.1 and 0.2 respectively.

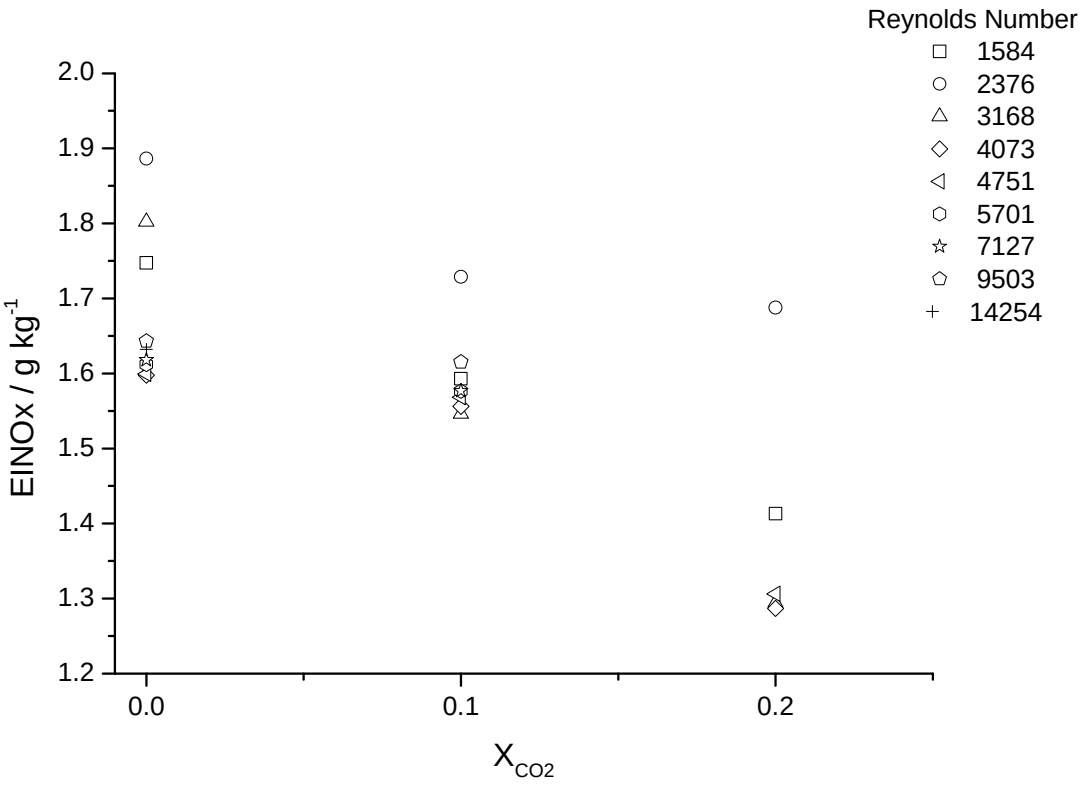

Fig. 11. Effect of CO_2 dilution on EINOx at different Reynolds numbers.

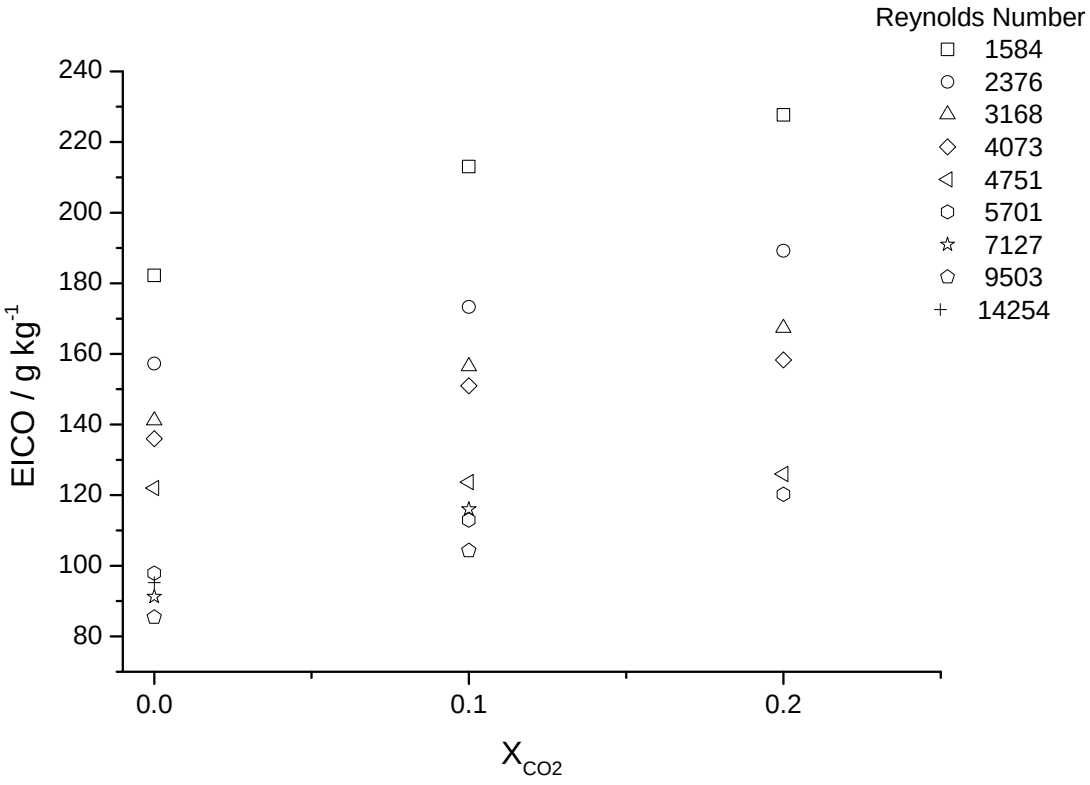

Fig. 12. Effect of CO_2 dilution on EICO at different Reynolds numbers.